Basic Characteristics and Durability of Low-Friction Sliding Bearings for Base Isolation

Masahiko Higashino [1)] Hiroki Hamaguchi [1)] Shigeo Minewaki [1)] Satoru Aizawa [1)]

1) *Structural Engineering Section, Takenaka Research and Development Institute, 1-5-1, Ohtsuka, Inzai, Chiba 270-1395, Japan.*

ABSTRACT

As base-isolated buildings become more popular, developments have been undertaken to comply with various needs such as those imposed by taller buildings or roomier architectural planning. Sliding bearings have gradually won engineering attention as these bearings can further elongate the natural period of the seismic isolation system, thereby enhancing seismic performance of the structures. This paper reports a series of studies on the low-friction sliding bearing developed by the writers. The writers conducted various tests to examine the characteristics of this device. Among all characteristics examined, durability was of major concern. The paper summarizes the experimental results that indicate how the device could maintain its initial characteristics after being subjected to a long-term high compressive stress and to cyclic horizontal load. An example of the application of the device to a high performance base isolation system is also discussed.

INTRODUCTION

Seismic isolation has become one of the core technologies for improving the performance of structures following the 1995 Hyogoken-Nanbu (Kobe) earthquake. Since that time the number of seismically isolated buildings has increased dramatically. Figure 1 shows the chronological increase of the number of buildings constructed with seismic isolation in Japan. Most seismically isolated buildings have employed rubber bearings to support the superstructure. Major engineering considerations for rubber bearings are the mean compressive stress and the expected maximum horizontal displacement. The limits of the compressive stress are directly associated with the upper limits of the natural period of the isolation system. Common upper limits of the natural period are about five seconds. This natural period allows a wide range of seismic-isolation buildings. But isolation technology has met another challenge, primarily from the architectural requirements of taller buildings with seismic-isolation and superstructures with more flexible architectural planning. These requirements demand a shift in structural design to allow better architectural design and better seismic performance. To meet these requirements, longer natural periods are needed for the seismic isolation system. Efforts to soften the rubber compound continue, but rubber whose shear modulus is smaller than 0.35MPa is not able to support high compressive stress. To overcome this limitation in rubber bearings, sliding bearings, which have a very small horizontal stiffness while being able to support large vertical load, are increasingly attracting engineers' interest. The number of seismically isolated buildings supported by sliding bearings is increasing. Figure 2 shows the chronological development of the number of buildings with sliding bearings after 1995. The number of seismically isolated buildings stabilized after 1997 at about 120 new designs each year. Figure 2 shows that the number of buildings with sliding bearings still continues to increase in recent years.

Sliding bearings were employed in the early stage of development of seismic isolation. A nuclear power plant with sliding bearings is one of the earliest applications [1]. The bearings used in the plant consisted of a sliding bearing and a rubber bearing joined in series. The rubber bearings were used to reduce the nearly rigid stiffness provided by the friction of the sliding bearings prior to sliding. Sliding bearings consisted of metals whose friction coefficient was 0.16 to 0.18. Recent applications employ sliding bearings using PTFE [2], popularly known as Teflon. Teflon is a trademark owned by Dupont. The friction coefficient between the PTFE and stainless steel is almost 0.1. Because of the very stable characteristics of PTFE, recent sliding bearings tend to use a combination of PTFE and stainless steel [3,4]. Compared to rubber bearings, the sliding bearing has a shorter history, and many of its characteristics remain to be examined. One major concern is its durability. Primary characteristics of sliding bearings before and after the ten years of service were examined by Nagashima, *et al*. [5]. In this report, the friction coefficient had increased by 20% after ten years. This increase is considered to be minor so the basic characteristics of the sliding bearing persist after supporting a vertical load for ten years.

Several seismically isolated buildings with sliding bearings were designed and constructed in the late 1980s. Most of the buildings employed

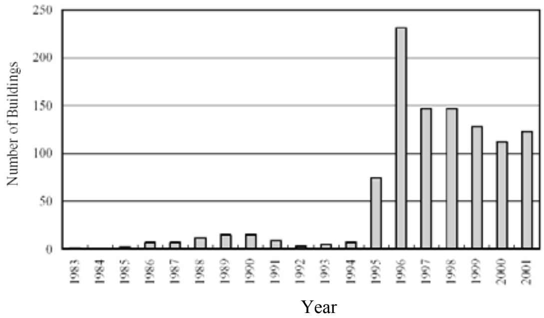

Fig. 1 Chronological development of seismically isolated buildings in Japan

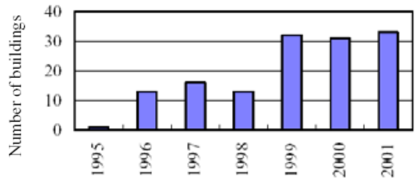

Fig. 2 Chronological development of buildings with sliding isolation bearings in Japan

PTFE and stainless steel plates. In combination with rubber bearings, the shear coefficient at the isolation layer yielded almost 0.08 in these cases [6]. As stated above, the requirements for seismic isolation have expanded beyond safety to more versatile applications such as taller buildings or freer architectural planning. To meet these requirements, less friction in sliding bearings is now needed.

The writers have conducted a wide range of tests to examine the characteristics of sliding bearings, whose friction is only 0.024 under the 15MPa compressive stress. By the end of 2002, the writers completed designs of about ten projects using low-friction sliding bearings. This paper summarizes the characteristics of these sliding bearings and presents an application to a real design project.

MAJOR CHARACTERISTICS OF THE DEVICE

The configuration of the proposed sliding bearings is shown in Fig. 3. The bearing consists

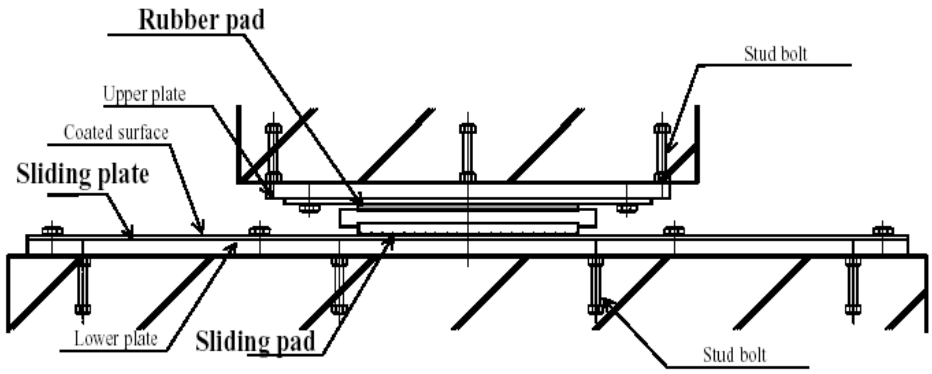

Fig. 3　Configuration of sliding isolation bearing developed

of the following components (listed from bottom to top): sliding plate, sliding pad, and rubber pad. The sliding plate is made of stainless steel, coated by heat-stiffened resin on its top. The sliding pad is made of PTFE with reinforcing additives. The friction coefficient between the sliding plate and the pad becomes less than 0.03 under a compressive stress of 15MPa. Note that the friction coefficient between stainless steel and PTFE is commonly about 0.1. The rubber pad used herein consists of a single layer of rubber, though many other sliding bearings use multi-layer rubber pads. The rubber pad is used to reduce the initial stiffness of the sliding bearing. The single layered rubber pad allows rotation above the sliding bearing and also decreases the vertical stiffness to a level achieved by common rubber bearing isolators.

A typical force-displacement relationship of this sliding bearing is shown in Fig. 4. The hysteresis is characterized by the static friction, dynamic friction, and initial stiffness. The initial stiffness is controlled by the rubber pad, and the other characteristics are controlled by the properties of the sliding pad and sliding plate. The friction coefficients are the functions of two parameters: the compressive stress and the velocity. Statistics on the effects of the compressive stress on the dynamic friction coefficient are shown in Fig. 5. Results of 131 full-scale tests having various diameters are plotted in this figure. The velocity between the sliding plate and the sliding pad was set at

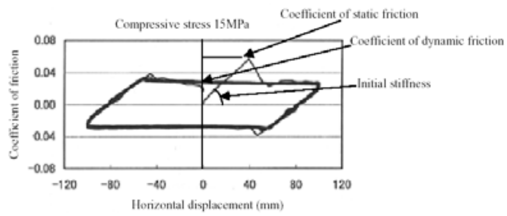

Fig. 4　Typical hysteresis of sliding isolation system

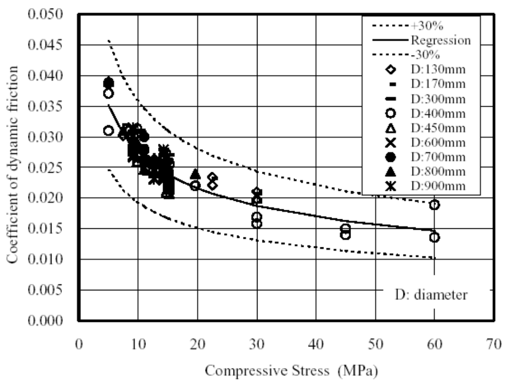

Fig. 5　Compressive stress dependency of coefficient of dynamic friction

0.15m/s. Regardless of the size of the bearings, the coefficients of dynamic friction are reasonably estimated by the following equation (within ±30%).

$$\mu_D \big|_{v=0.15} = 0.0618\,\sigma^{-0.351} \tag{1}$$

where μ_D is the coefficient of dynamic friction and σ is the compressive stress between the sliding plate and the sliding pad with units of

MPa.

Friction is considered to be a result of the digging effect and adhesive effect. In recent studies of tribology, the adhesive effect is considered to be dominant [7]. The adhesive force is considered to be proportional to the true contact area (Fig. 6).

$$F_{adh} \propto A\,s \tag{2}$$

where A is the true contact area and s is the shear strength per unit area. Based on Hertz's theory, the true contact area is proportional to 2/3 power of the vertical force; hence the friction force is given as follows [7]:

$$F_{adh} \propto P^{2/3} \tag{3}$$

where P is the vertical load. The coefficient of friction will be as follows:

$$\mu \approx \frac{F_{adh}}{P} = k\,P^{-1/3} \tag{4}$$

The exponent of 0.351 in Eq. (1) is close to 1/3 shown in Eq. (4), indicating a close correlation between the two equations.

The velocity dependency of the coefficient of dynamic frictions is shown in Fig. 7. The compressive stress is set at 15MPa. The number of test plots shown is 38 in this figure. Regardless of the size of the bearings, the coefficient of dynamic frictions is reasonably expressed by the following equation:

$$\mu_D\big|_{\sigma=15} = 0.0307\,v^{0.132} \tag{5}$$

where v is the velocity between the sliding plate and sliding pad with units in m/s. Combining Eqs. (1) and (5), we obtain the following relationship:

$$\mu_D = 0.0793\,\sigma^{-0.351}\,v^{0.132} \tag{6}$$

The compressive stress dependency of the coefficient of static friction is shown in Fig. 8. Assuming the mechanisms are the same for both the dynamic and static friction, a regression line based on Eq. (5) and ±30% range are also shown in Fig. 8. The equation given by regression is as follows:

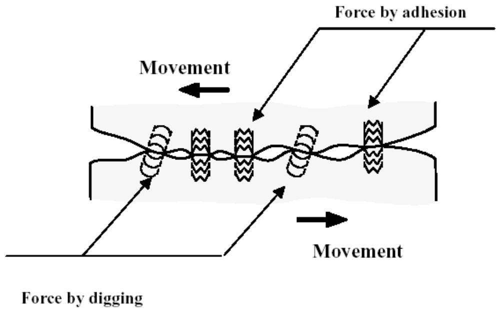

Fig. 6 The model of friction mechanism

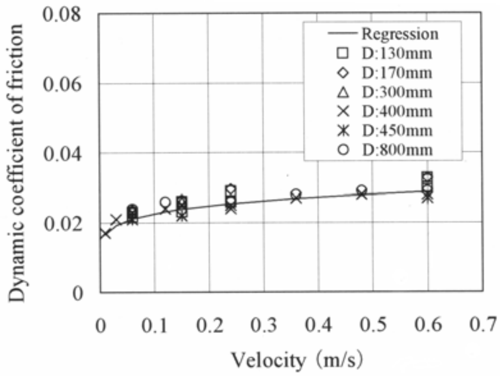

Fig. 7 The velocity dependency of coefficient of dynamic friction

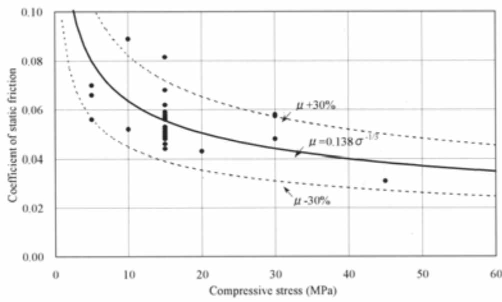

Fig. 8 Compressive stress dependency of coefficient of static friction

$$\mu_S\,|_{v=0.15} = 0.138\,\sigma^{-1/3} \tag{7}$$

Since the static friction corresponds to the peak value, it has larger dispersion as compared to the dynamic friction.

DURABILITY FOR SLIDING DISTANCE

The durability of the sliding bearing is considered in two aspects:

(1) Durability with respect to the total sliding distance: This distance is defined as the total excursion of the horizontal displacement. This has the effect of wearing the sliding material.

(2) Durability under a long-term vertical load; this causes sticking between the pad and plate.

The durability associated with (1) can be tested in the laboratory. The experimental result for a 300mm diameter with 2mm thick sliding pad and a 20mm diameter with 1mm thick sliding pad are shown in Fig. 9. The coefficient of dynamic friction increases gradually over the 60m sliding distance for the 300mm specimen with 30MPa compressive stress. For the 15MPa compressive stress, changes in the friction coefficient before 180m of sliding distance were not observed for the 300mm and 20mm specimens. The distance, 180m, is much larger than the sliding distance induced by strong earthquakes, which is commonly not greater than 3 to 4m for each earthquake response. These observations indicate that the sliding bearing has enough durability with respect to the sliding distance. The commercial models are designed to be used under 15MPa compressive stress based on this result. The difference in the absolute value between a 20mm specimen and a 300mm specimen resulted from the difference of aspect ratios [8], defined as the diameter of sliding pad divided by its thickness. The 20mm specimen had a larger true contact area compared to the 300mm specimen. As seen in Figs. 5 and 7, the full-scale specimens show consistent friction coefficients regardless of size. This suggests that the true contact area of the sliding pad with a large aspect ratio is nearly constant in terms of the ratio of the apparent surface area.

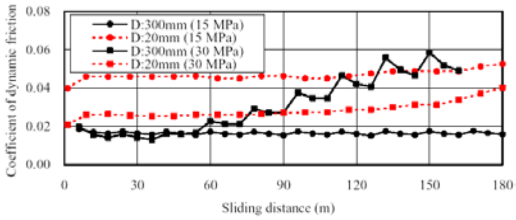

Fig. 9 Durability test results of sliding bearings

ACCELERATED AGING TEST BY SCALED MODEL

Durability under the long-term vertical load is difficult to examine since we have to wait for several decades to acquire true experimental results. The writers conducted three tests to envisage the reality in the future. The tests conducted are as follows:

(1) Accelerated aging test by a scaled model.

(2) Vertical load test for 60 hours in the laboratory.

(3) Building pushing test before and after six months from completion.

Changes in friction coefficient by aging are considered to be the result of the changes in adhesion characteristics between the sliding pad and sliding plate. The materials used here are the coated stainless steel and PTFE. Since the chemical characteristics of the coating material and PTFE have virtually no aging effects, the change in friction coefficient is attributed primarily to the creep of materials and resultant increase in the contact area between the pad and plate. Material creep, particularly for rubber bearings, is often estimated from the model using Arrhenius's theory [11,12]. Also, we observed that the friction model based on the true contact area between the sliding plate and sliding pad agreed reasonably with the experimental results in Section "Major characteristics of the device." If these two models are considered applicable, the change of friction coefficient may be predicted from the accelerated aging test. Although this method contains many assumptions, there are few alternatives.

The specimens and test conditions are shown in Table 1. As shown in the table, both the real time-scale test and accelerated aging test were conducted. The compressive stress in the tests was set at 15MPa. Static friction and dynamic friction coefficients were measured in the tests. Coefficients for the static friction are shown in Fig. 10, and those of the dynamic friction are shown in Fig. 11. In Fig. 10, the increase of the static friction coefficient is notable. The increase of static friction over time has been expressed by Rabinowicz [9]:

$$\mu_S = \mu_0 + k\, t^{0.1} \tag{8}$$

where t is the time, measured in years. Using this theory, we obtain the following equation by regression analysis:

$$\mu_S = 0.05 + 0.016\, T^{0.1} \tag{9}$$

where T is time in years. No noticeable change in the coefficient of dynamic friction is seen in Fig. 11. This result indicates that creep affects the static friction. The coefficients of dynamic friction remained almost unchanged. This reveals that when movement cuts the previous contact between the pad and plate and shifts to a new combination between the pad and plate, the friction becomes almost the same as the original.

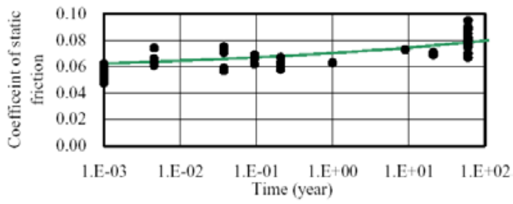

Fig. 10 Aging effect in coefficient of static friction

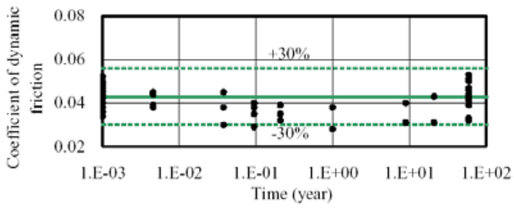

Fig. 11 Aging effect in coefficient of dynamic friction

Table 1 Specimens and testing conditions for accelerated aging tests

Specimen	Time									Velocities
Dimension*	No.	Initial	40hr	330hr	830hr	1830hr	1yr	9yr	21yr	60yr	(mm/s)
40-2	1	R	R	R							10, 100
40-2	1	R	R	R	R	R					10, 100
40-2	1	R								A	10, 100
40-2	1	R		A	A	A	A	A	A	A	10, 100
35-3	12	R								A	100

R: Tested in real time, A: Tested in accelerated time *: diameter (mm) – thickness (mm)

60 HOURS VERTICAL LOAD IMPOSITION

Examinations shown above indicated that creep has a noticeable effect on the coefficient of static friction. To further investigate the effect of creep and long-term vertical load, tests to measure the friction coefficient before and after the imposition of vertical load for 60 hours were conducted. The test apparatus is shown in Fig. 12. The capacities of the dynamic actuator and the static jack adopted for horizontal and vertical load are shown in Table 2 and Table 3, respectively. Major dimensions of the specimen are shown in Table 4.

Table 2 Capacity of dynamic actuator

Maximum force	1,000kN
Maximum stroke	0.5m both direction (1.0m peak to peak)
Maximum velocity	1.0m/s
Maximum acceleration	10m/s^2

Table 3　Capacity of static jack

Maximum compression force	20,000kN
Maximum tensile force	10,000kN
Maximum stroke	1.0m peak to peak

Table 4　Dynamic friction in building pushing test

Loading step	First test	Second test	Designed value
A to B	0.028	0.023	Upper limit: 0.042 Lower limit: 0.020 Test result in the mill: 0.023
C to D	0.023	0.020	
D to E	0.024	0.021	
F to G	0.024	0.018	
Average	0.025	0.021	

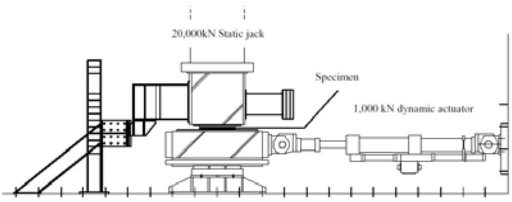

Fig. 12　Full scale testing apparatus

Figure 13 shows the force-displacement relationships before and after the imposition of vertical load for 60 hours. Horizontal load was applied with a constant velocity of 0.01m/s. By subtracting the friction of the testing apparatus itself, the coefficient of static friction was measured as 0.043 for the initial test. The coefficient of dynamic friction obtained from this test was determined with a very small velocity. The coefficient with a large velocity will be discussed at the end of this section. The specimen was subjected to a static vertical load of 7,500kN, which corresponds to a 15MPa compressive stress at the sliding surface for 60 hours after initial loading tests. The period of 60 hours was chosen from previous observation, which showed that creep was stabilized after 20 hours. The coefficient of static friction measured after 60 hours was 0.046. These results show that the coefficient of static friction remained almost the same even after 60 hours of vertical load. Referring to Eq. (9), the increase in the coefficient of static friction after 60 hours

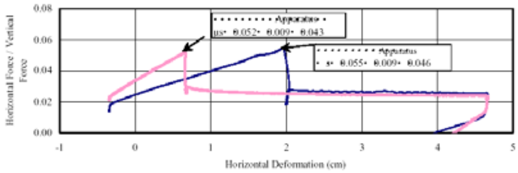

Fig. 13　Static friction before and after 60 hours of vertical load

is about 6%. The test results increased 7% from 0.043 to 0.046, indicating good correlation between the test and the prediction.

Creep in the PTFE measured during the 60 hours of vertical load is shown in Fig. 14. The creep was stabilized after 20 hours for this test as well, and converged at about 0.13mm. Figure 15 shows photos of the pressure distribution measured by pressure sensing sheets before and after the 60 hours of vertical load. The pressure distributions are nearly the same between the two conditions. Since a creep of 0.1mm is very small, the value may have to be examined in future tests. But qualitatively, the creep seems to have almost converged after 20 hours. Considering the very small change in pressure distribution (Fig. 15), we can reasonably conclude that increase in the true contact area after 60 hours loading is minimal and most of the measured creep occurred within the PTFE pad.

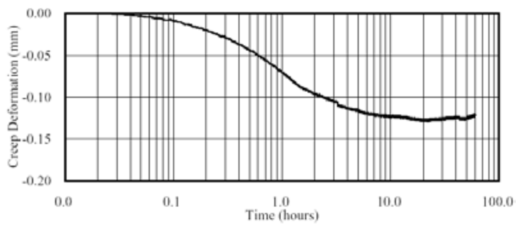

Fig. 14　Creep in PTFE by 60 hours of vertical load

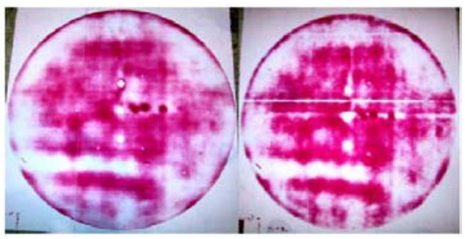

Before　　After

Fig. 15　Pressure distribution before and after 60 hours of vertical load

To examine possible changes in the coefficient of dynamic friction, cyclic loading tests were conducted. Figure 16 shows cyclic loading test results before and after the 60 hours of vertical load. By subtracting friction in the test apparatus (a 0.009 friction coefficient), the initial coefficient of dynamic friction was given as 0.021 and that measured after 60 hours was 0.025. The increase was almost 20%. However, by the time of the second test (after 60 hours), the specimen had experienced a total sliding distance of 80m. Part of the 20% increase was attributed to the wear of the material. Thus, we may reasonably conclude that the increase was relatively small.

CONSTRUCTION OF BUILDING WITH SLIDING BEARINGS

Ten building projects in which the developed sliding bearings were adopted had passed peer review by the end of the year 2002. All of the buildings had flexible superstructures, including high-rise buildings, old weak buildings to be retrofitted, and structures with very thin columns. Different types of sliding bearings have also been developed in Japan, and the number of buildings designed with the sliding bearings is increasing (Fig. 2), as noted earlier.

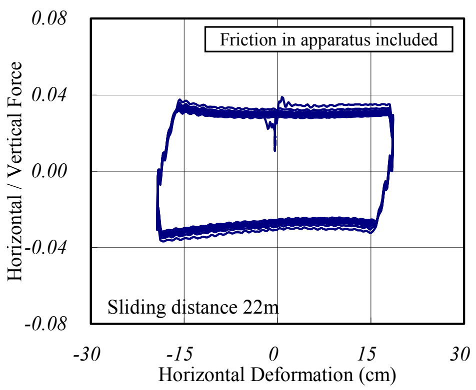

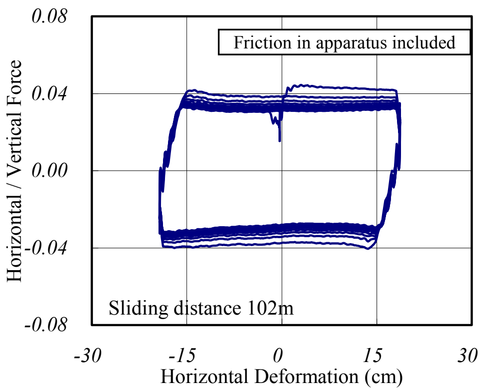

Fig. 16 Hysteresis before and after 60 hours vertical load

The building introduced in the paper was completed in 2000. It has three floors with a maximum height of 11.0m. The total weight of the superstructure is 3,000ton (300MN). The building has no columns or girders and uses instead thin walls and flat slabs. The system was chosen based on architectural requirements to allow flexible change in planning. This thin superstructure system was realized only through the use of a long natural period seismic isolation system into which low friction sliding bearings are incorporated.

The layout of the seismic isolation devices is shown in Fig. 17. The weight of the building is supported solely by the sliding bearings. Two rubber bearings provide horizontal restoring forces, but do not sustain any vertical load (Fig. 19). The overall horizontal force-displacement relationship of the isolation system is shown in Fig. 20. The natural period estimated based on the secant stiffness at a horizontal displacement of 400mm is larger than 5 seconds. The structural plan at the first floor is shown in Fig. 21. Free open space, achieved by a smaller number of walls, is assured in this plan. Figure 22 shows the view of the completed building.

Figure 23 shows the maximum response distributions along the height, obtained for the earthquake motion shown in Fig. 24. The duration and maximum acceleration of the motion are 120 seconds and 4.38m/s^2, respectively. Although the building has a soft superstructure, the displacement response shows a rigid profile. The acceleration responses are not greater than 1m/s^2 for all floor levels. The outstanding performance of the isolation system is notable in this example.

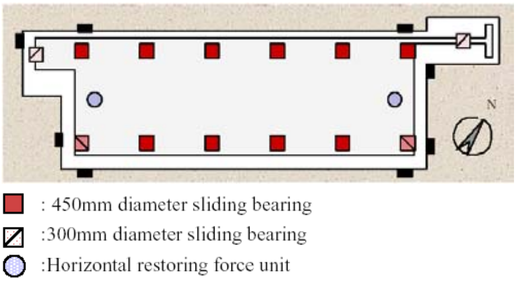

Fig. 17 The layout of devices in isolation interface

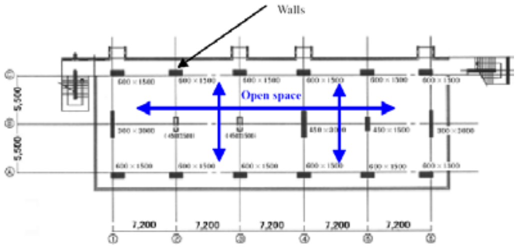

Fig. 21 Structural plan (First floor)

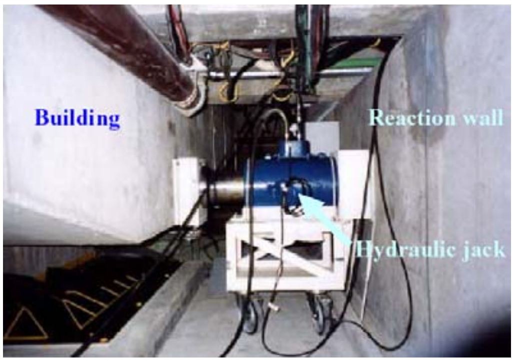

Fig. 18 The view of horizontal loading system

Fig. 22 View of the building

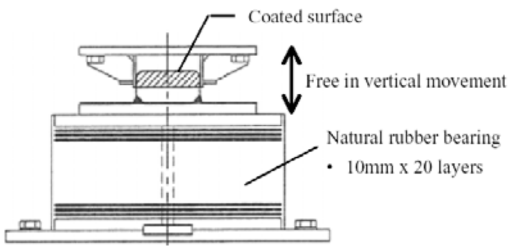

Fig. 19 Configuration of horizontal restoring force unit

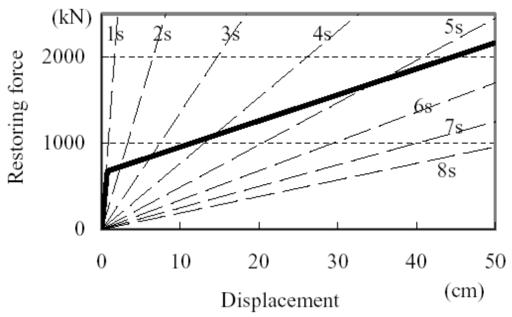

Fig. 20 Designed force-displacement relationship of isolation interface

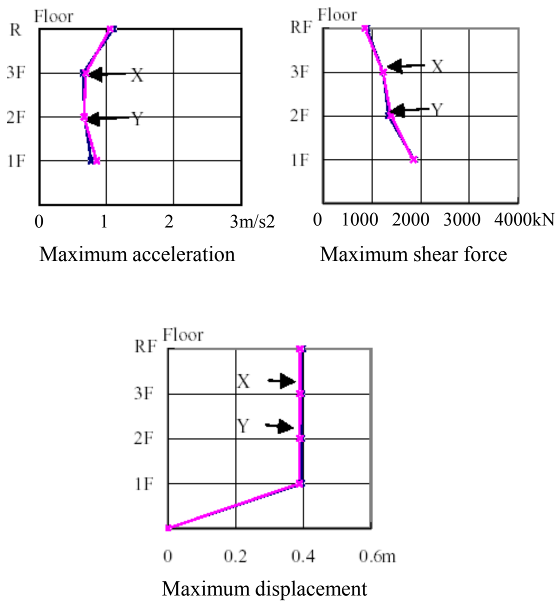

X: Longitudinal direction of building
Y: Transverse direction of building

Fig. 23 Maximum response profile

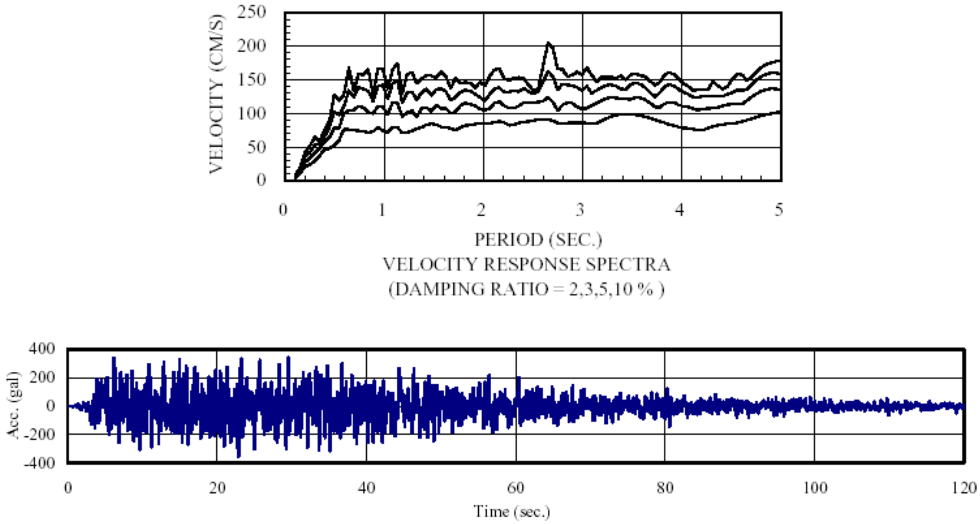

Fig. 24 Earthquake used in response analysis (BCJ-Level2 artificial earthquake)

BUILDING PUSH TESTS BEFORE AND AFTER SIX MONTHS

In November 1999, the structural system was almost completed. The first push test was conducted in February 2000 (by that time the sliding bearings had carried the weight of the building for about three months), and the second push test was conducted in August 2000. The building was pushed at the base-isolation level by two 2.0MN hydraulic jacks. A view of the load-applying system is shown in Fig. 18. The horizontal force-displacement relationships obtained from the two push tests are shown in Fig. 25 for the initial range of loading. The coefficients of static friction for the first and second tests were 0.041 and 0.044, respectively. The increase of the coefficient of static friction was almost 7%. According to Eq. (8), change in friction between three and nine months is about 7%, which shows a very good correlation between the test and the prediction.

Figure 26 shows a comparison of the overall force-displacement hysteretic curves obtained from the two tests. The dynamic friction obtained from the second test (from 0.018 to 0.023) is rather small compared to that from the first test (from 0.027 and 0.029). The friction coefficients measured for each loading step are summarized in Table 4. These results indicate that the dynamic friction did not change notably after six months. This suggests that the difference of three months and six months had a small effect to the change in the coefficient of dynamic friction. As evidenced in the previous sections, the coefficient of friction tends to change during the initial application of vertical load; the friction is likely to stabilize after 3 months.

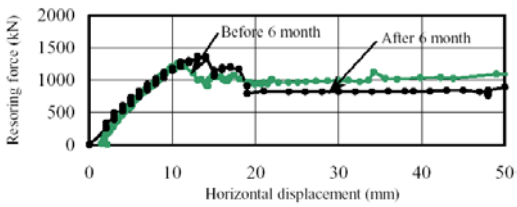

Fig. 25 Force-displacement relationship of isolation interface of the building (Static friction)

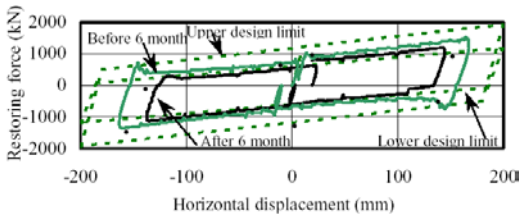

Fig. 26 Combined hysteresis of isolation interface of the building

CONCLUSIONS

The fundamental characteristics and durability of a low-friction sliding bearing are studied. Primary findings obtained from this study are as follows:

(1) The coefficient of dynamic friction was found to be proportional to a –0.351 power of the compressive stress, which agreed well with the theory by Hertz.
(2) The coefficient of dynamic friction was found to be proportional to a 0.132 power of the velocity between the sliding pad and sliding plate.
(3) For a standard compressive stress of 15MPa, the coefficient of dynamic friction remained almost the same up to a sliding distance of 180m.
(4) Accelerated aging tests showed that the coefficient of static friction increases by a 0.1 power of the time, but the coefficient of dynamic friction is independent of time.
(5) No noticeable change in dynamic friction was observed after imposing a constant vertical load corresponding to a compressive stress of 15MPa for 60 hours. This observation was also supported by the push tests applied to the real building.
(6) No noticeable change in static and dynamic friction was observed after 6 months of service.

All the experimental results indicated that the developed low-friction sliding bearings have very stable characteristics for use in seismic isolation. The standard coefficient of dynamic friction is about 0.024 at a compressive stress of 15MPa, and this low friction makes it possible to achieve a base-isolation with a natural period longer than 5 seconds. With this level of natural period, higher performance of seismic isolation can be achieved allowing for freer architectural design, more effective retrofits of weak structures, freer design of high-rise, etc. These experimental results are promising for the application of low-friction sliding bearings to isolated buildings.

ACKNOWLEDGEMENT

The push test of the example building presented in this paper was conducted as part of the project named "House Japan," supervised by the New Energy Developing Organization and funded as the third supplemental budget of 1998 by the Ministry of International Trade and Industry. The low-friction sliding bearing is a product of NTN Engineering Plastic Corporation.

REFERENCES

1. Jolivet, F. and Richli, M. (1977). "A seismic foundation system for nuclear power stations", Proc. 4SMiRT paper K9/2.
2. K. Kitazawa, *et al*. (1997). "Base isolation system with sliding bearings, Part 1 Outline of the system", *Proc. AIJ Annual Meeting*, Vol. B, p. 817.
3. Emori, J. Yamanaka, H. *et al*. (1998). "An experimental study on basic mechanical characteristics of elastic sliding bearing," *Proc. AIJ Annual Meeting*, Vol. B-2, p. 487.
4. Nakamura, S. Kitamura, Y., *et al*. (1998). "Seismic isolation system using rubber bearings and sliding bearings, Part 1 Shear loading test under constant compression," *Proc. AIJ Annual Meeting*, Vol. B-2, p. 501.
5. Nagashima, I., *et al*. (1998). "Experimental evaluation of aging effects on properties of a building with sliding base isolation system," *Proc. 10JEES*, p. 2659.
6. A. Kono (2001). "Kobe North Municipal Fire Station," MENSHIN No.32 2001/5, p.15
7. Bowden, F.P. and Tabor, D. (1954). "The friction and lubrication of solids," Clarendon Press, Oxford.
8. Hamaguchi, H. and Higashino, M. (2000). "Development of low-friction factor sliding isolation device," *12WCEE*, 2135/6/A.
9. Rabinowitz, E. (1958). *Proc. Roy. Soc*., B71, p. 668.
10. Hamaguchi, H., Higashino, M. and *et al*. (2001). "Aged deterioration in the coefficient of friction of sliding bearings," *AIJ Annual Meeting*, Vol. B-2, p. 645.
11. Fukahori, Y. (2000). "The dynamics of polymers," Gihodo Shuppan (in Japanese).
12. Zhurkov, S.N. and Tomashevsky, E.E. (1966). "Physical basis of yield and fracture", Institute of Physics & the Physical Society, p. 200.